RAA 2016 Vol. **16** No. **3**, 38 (6pp) doi: 10.1088/1674–4527/16/3/038
http://www.raa-journal.org *http://iopscience.iop.org/raa*

***R**esearch in*
***A**stronomy and*
***A**strophysics*

Estimate of an environmental magnetic field of fast radio bursts

Wei-Li Lin and Zi-Gao Dai

School of Astronomy and Space Science, Nanjing University, Nanjing 210023, China; *dzg@nju.edu.cn*
Key Laboratory of Modern Astronomy and Astrophysics (Nanjing University), Ministry of Education, Nanjing 210023, China

Received 2015 March 30; accepted 2015 October 29

Abstract Fast radio bursts (FRBs) are a type of newly-discovered transient astronomical phenomenon. They have short durations, high dispersion measures and a high event rate. However, due to unknown distances and undetected electromagnetic counterparts at other wavebands, it is difficult to further investigate FRBs. Here we propose a method to study their environmental magnetic field using an indirect method. Starting with dispersion measures and rotation measures (RMs), we try to obtain the parallel magnetic field component $\overline{B}_{||}$ which is the average value along the line of sight in the host galaxy. Because both RMs and redshifts are now unavailable, we demonstrate the dependence of $\overline{B}_{||}$ on these two separate quantities. This result, if the RM and redshift of an FRB are measured, would be expected to provide a clue towards understanding an environmental magnetic field of an FRB.

Key words: radio continuum: general — pulsars: general — galaxies: magnetic fields — Galaxy: structure

1 INTRODUCTION

Fast radio bursts (FRBs) are a type of transient radio pulse mostly detected in the high Galactic latitude region. Lorimer et al. (2007) reported a 5 ms radio pulse with a high dispersion measure in excess of the Galactic contribution, which suggested that FBRs have a cosmological origin. They also found that it was observationally unrepeatable and not associated with any published gamma-ray bursts (GRBs) or supernovae. Thornton et al. (2013) listed four FRBs and obtained a high event rate of about 10^{-3} $\mathrm{gal}^{-1}\ \mathrm{yr}^{-1}$, which is inconsistent with the rates of GRBs, SNe or neutron star mergers. These observational properties of FRBs indicate their unusual origins.

So far, several models have been proposed to explain FRBs at cosmological distances. Soft gamma-ray repeaters could produce FRBs due to tearing mode instability in the magnetar magnetosphere (Popov & Postnov 2007; Thornton et al. 2013). Another promising candidate is the coherent emission generated by energy loss from magnetic breaking in the evolution process, e.g., that occurs after the merger of double neutron stars (Totani 2013), the merger of binary magnetized white dwarfs (Kashiyama et al. 2013), or the collapse of a supramassive neutron star (Falcke & Rezzolla 2014). In addition, the steep decays after the shallow decay phases during X-ray afterglows of some GRBs imply they are collapses of supramassive neutron stars, leading to the suggestion by Zhang (2014) of a connection between FRBs and some GRBs. Thus FRBs would provide a new possibility to explore activities associated with these compact objects. However, it is difficult to understand FRBs in a direct way when any electromagnetic counterpart at other wavebands remains undetected. In this paper, we investigate the dependence of an environmental magnetic field of FRBs by using dispersion measures (DMs) and rotation measures (RMs).

This paper is organized as follows. In Section 2, we show that FRBs are extragalactic sources by comparing DMs of the Milky Way (MW) with the total DMs. In Sections 3 and 4, we attempt to study the contribution from MW and the intergalactic medium (IGM) to the total DMs and RMs of FRBs. In particular, when considering the MW component, we discuss some typical models of the Galactic magnetic field (MF). In Section 5, we obtain a formula describing $\overline{B}_{||}$, i.e. the environmental MF component of FRBs averaged along the line of sight, and provide further discussion.

2 FRBS, THE EXTRAGALACTIC ORIGINS

The DM is defined from the delay in arrival times of radio waves at two observed frequencies of $\nu_{1,\mathrm{obs}}$ and $\nu_{2,\mathrm{obs}}$ (Rybicki & Lightman 1979; Deng & Zhang 2014)

$$\begin{aligned}\Delta t_{\mathrm{obs}} &= \Delta t(1+z) \\ &= \frac{e^2}{2\pi m_e c}\left(\frac{1}{\nu_{1,\mathrm{obs}}^2}-\frac{1}{\nu_{2,\mathrm{obs}}^2}\right)\int\frac{n_e}{1+z}dl, \quad (1)\end{aligned}$$

where n_e is the free-electron number density of the medium through which radio waves propagate, z is the redshift and l is the path length in the intervening medium.

The RM is extracted from the formula for Faraday rotation angle (Rybicki & Lightman 1979)

$$\Delta\varphi = \frac{2\pi e^3}{m^2c^2\omega_{\rm obs}^2}\int\frac{n_eB_{||}}{(1+z)^2}dl, \quad (2)$$

where $\omega_{\rm obs}$ is the angular frequency in the observer frame and $B_{||}$ means the MF component along the line of sight. Then we introduce the general definition of observed DM and RM

$$\begin{cases} {\rm DM} &= \int\frac{n_e}{1+z}dl, \\ {\rm RM} &= 0.81\int\frac{n_eB_{||}}{(1+z)^2}dl, \end{cases} \quad (3)$$

where n_e is in units of cm^{-3}, l is in pc, and $B_{||}$ is in μG. From the above definition, DM (in pc cm^{-3}) actually represents the distance with a known electron distribution. Therefore, if the electron number density n_e and the distance are known, RM (in rad m^{-2}) reflects the MF component along the line of sight.

There remains a problem of how to measure the luminosity distances of FRBs when their host galaxies have not yet been detected. However, we can use DM as a proxy for distance to judge whether FRBs are in the MW.

In Table 1, we show seven FRBs with observed ${\rm DM_{tot}}$ (Thornton et al. 2013; Burke-Spolaor & Bannister 2014; Spitler et al. 2014; Petroff et al. 2015) and ${\rm DM_{MW}}$ from the code that is part of the NE2001 model (Cordes & Lazio 2002, 2003). Assuming that the contribution of the source is small enough, ${\rm DM_{tot}}$ beyond ${\rm DM_{MW}}$ indicates that FRBs originate from extragalactic sources.

We can divide DM and RM of FRBs into several spatial components, including the MW component, the IGM component, and the host galaxy component with an insignificant source component

$$\begin{aligned} {\rm DM_{tot}} &= {\rm DM_{MW}} + {\rm DM_{IGM}} + {\rm DM_{host}} \\ &= \int_{\rm MW} n_e dl + \int_{\rm IGM}\frac{n_e}{1+z}dl \\ &\quad + \frac{1}{1+z_{\rm host}}\int_{\rm host} n_e dl, \end{aligned} \quad (4)$$

$$\begin{aligned} {\rm RM_{tot}} &= {\rm RM_{MW}} + {\rm RM_{IGM}} + {\rm RM_{host}} \\ &= 0.81\int_{\rm MW} n_eB_{||}dl + 0.81\int_{\rm IGM}\frac{n_eB_{||}}{(1+z)^2}dl \\ &\quad + 0.81\,\frac{1}{(1+z_{\rm host})^2}\int_{\rm host} n_eB_{||}dl. \end{aligned} \quad (5)$$

3 CONTRIBUTION FROM THE MW

The electron density distribution of MW is well described by the NE2001 model, which can be integrated along the path to obtain ${\rm DM_{MW}}$. It is widely accepted that the Galactic MF consists of two independent parts: a disk field and a halo field. They have been identified from the RMs of pulsars near the Galactic plane and from extragalactic radio sources respectively.

The disk field is arranged parallel to the Galactic plane since the vertical component is about one order of magnitude smaller than the horizontal one (Han & Qiao 1994). The general horizontal structure follows a spiral pattern that can be divided into two classes, axi-symmetric spiral (ASS) and bi-symmetric spiral (BSS) (e.g., Han et al. 1999, 2006; Sun et al. 2008). Han et al. (1999, 2006) showed that there are field reversals near the spiral arms, which support the BSS model. However, Sun et al. (2008) preferred the ASS model because this model matches the RM distribution well between $l = 100^\circ$ and $l = 120^\circ$ at low latitudes. We adopt two typical models, the ASS model plus reversals in rings (hereafter Disk I) and BSS model (hereafter Disk II; Sun et al. 2008) and show the field configurations in Figure 1.

The sign antisymmetry of extragalactic RMs about the Galactic plane indicates that the halo field is distributed counterclockwise above the Galactic plane and clockwise below the plane (Han et al. 1997). But as a whole, RM profiles in the middle latitude region versus longitude show an asymmetric MF structure with respect to the Galactic plane and the Galactic center, respectively (Sun et al. 2008), which inspires different forms of fitting to the field distribution. We consider four halo models collected by Mao et al. (2012), a double-torus halo field (Prouza & Šmída 2003; hereafter Halo I), a spiral configuration (Jansson et al. 2009; hereafter Halo II), a toroidal structure plus vertical component (Ruiz-Granados et al. 2010; hereafter Halo III) and a toroidal field in the central region (Mao et al. 2012; hereafter Halo IV). It should be noted that instead of the NE2001 model, Halo IV is used with a simple electron density distribution as Mao et al. (2012) offered. The different halo field configurations are shown in Figure 2.

Since the MF is modeled by components of the disk and halo, the two disk models and four halo models are actually combined into eight kinds of field configurations. We show the RMs in different models in Figure 3 and list the ${\rm RM_{MW}}$ of all the configurations along the directions of FRBs in Table 2.

4 CONTRIBUTION FROM IGM

Planck Collaboration et al. (2014) provided the cosmological parameters of $\Omega_m = 0.315$, $\Omega_\Lambda = 0.685$, $h = 0.673$ and $\Omega_b = (0.0458, 0.0517)$. We adopt the average value 0.0488 for Ω_b. The mean free-electron density in intergalactic space can be described as (e.g., Inoue 2004)

$$n_e = \frac{3H_0^2\Omega_b}{8\pi Gm_p}\chi_e(z)(1+z)^3. \quad (6)$$

Since the neutral fraction of IGM at $z < 5.5$ is less than 10^{-4}, we consider all baryons as being fully ionized, i.e. the ionization degree $\chi_e(z<1) = 1$ (e.g., Fan et al. 2006).

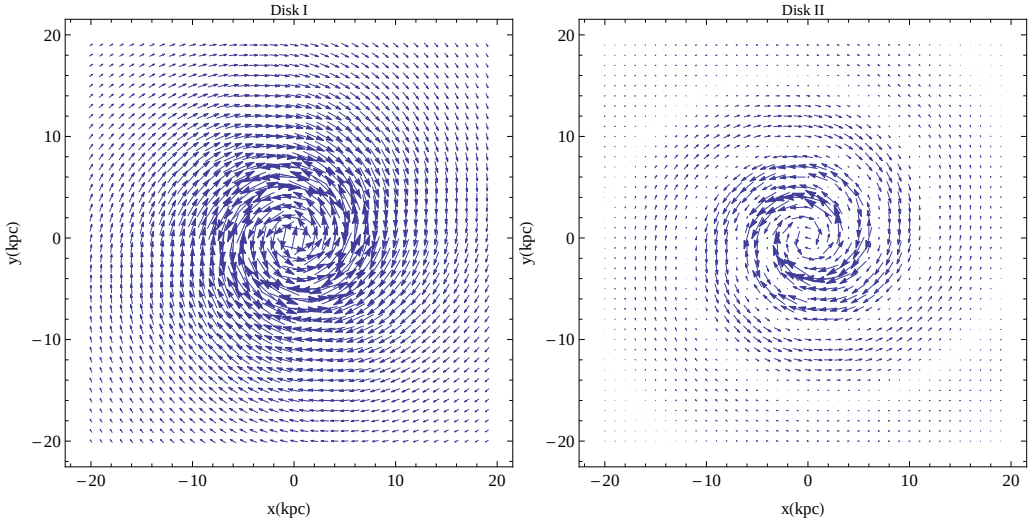

Fig. 1 Two disk field configurations at 1 kpc above the Galactic plane as seen from the north Galactic pole.

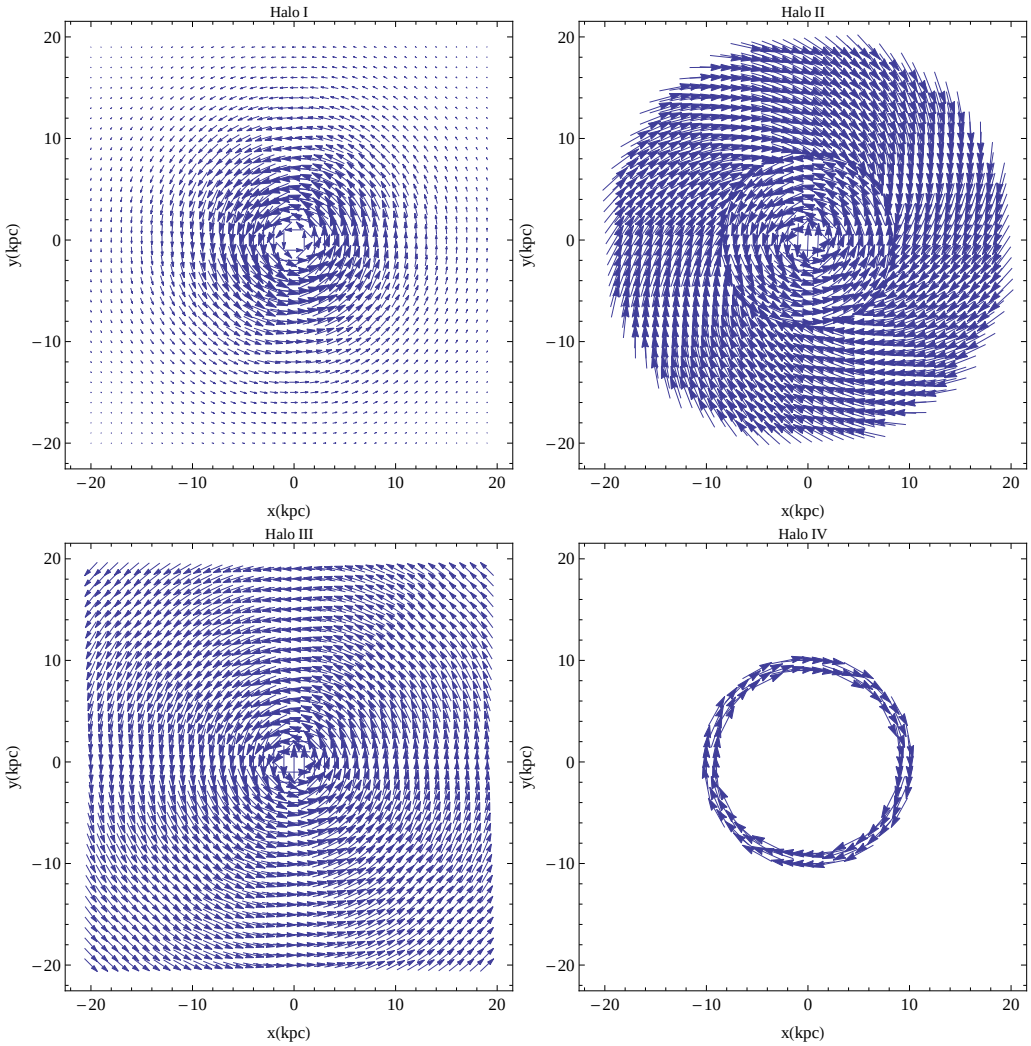

Fig. 2 Four halo field configurations at 1 kpc above the Galactic plane as seen from the north Galactic pole.

Table 1 We list information about some FRBs that was acquired through observations. This includes Galactic longitude (l) and latitude (b), and DM. We can calculate $\mathrm{DM_{MW}}$ and DM of the extragalactic contribution ($\mathrm{DM_E}$).

FRB	011025	110220	110627	110703	120127	121102	140514
$l(^\circ)$	356.6	50.8	355.8	81	49.2	175.0	50.8
$b(^\circ)$	–20.0	–54.7	–41.7	–59	–66.2	–0.223	–54.6
$\mathrm{DM_{tot}(pc\ cm^{-3})}$	790	944.38	723	1103.6	553.3	557.4	562.7
$\mathrm{DM_{MW}(pc\ cm^{-3})}$	110	34.9	47.6	32.3	32	188.5	34.9
$\mathrm{DM_E(pc\ cm^{-3})}$	680	909	675	1071	521	368.9	527.8

Table 2 $\mathrm{RM_{MW}}$ $(\mathrm{rad\ m^{-2}})$ of FRBs by calculating Galactic MF models listed above. Four sets of parameters for Halo I have been applied to obtain the $\mathrm{RM_{MW}}$ (Sun et al. 2008; Jansson et al. 2009; Sun & Reich 2010; Pshirkov et al. 2011).

FRB	011025	110220	110627	110703	120127	121102	140514
Disk I+Halo I (Sun et al. 2008)	11.9	–31.9	0.545	–29	–19.3	31.2	–32
Disk II+Halo I (Sun et al. 2008)	6.93	–30.3	1.15	–28.4	–18.4	6.56	–30.4
Disk I+Halo I (Jansson et al. 2009)	2.14	–21.5	–1.5	–20.5	–13.4	32.1	–21.6
Disk II+Halo I (Jansson et al. 2009)	–0.232	–20.4	–0.299	–20	–12.8	7.44	–20.5
Disk I+Halo I (Sun & Reich 2010)	2.69	–19.8	–1.9	–17.7	–12.3	31.9	–19.8
Disk II+Halo I (Sun & Reich 2010)	–2.29	–18.2	–1.29	–17.1	–11.4	7.26	–18.2
Disk I+Halo I (Pshirkov et al. 2011)	2.38	–22.1	–1.61	–20.3	–13.7	31.5	–22.1
Disk II+Halo I (Pshirkov et al. 2011)	–2.6	–20.5	–1	–19.7	–12.8	6.85	–20.5
Disk I+Halo II	4.56	–24.2	–1.76	–22.2	–14.9	32.1	–24.3
Disk II+Halo II	2.19	–23.1	–0.513	–21.7	–14.2	7.44	–23.2
Disk I+Halo III	12.0	–20.8	4.1	–19.1	–11	32.1	–20.9
Disk II+Halo III	6.98	–19.2	4.8	–18.5	–10.1	7.46	–19.3
Disk I+Halo IV	–1.64	–11.7	–1.6	–11.1	–7.4	37.6	–11.7
Disk II+Halo IV	–3.69	–10.8	–1.5	–10.7	–6.7	0.772	–10.9

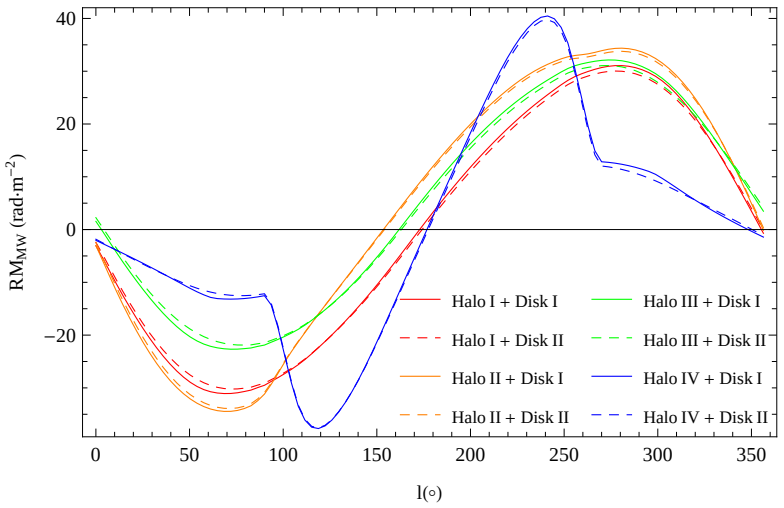

Fig. 3 $\mathrm{RM_{IGM}}$ profiles averaged for Galactic latitude intervals between -40° and -70°.

As for the intergalactic MF, it is reasonable to consider that the field is frozen in the IGM (Vallee 1975), which means

$$B = B_0(1+z)^2, \tag{7}$$

where B_0 roughly ranges from 10^{-9} μG to 10^{-3} μG (e.g., Schleicher & Miniati 2011; Neronov & Vovk 2010; Dolag et al. 2011; Dermer et al. 2011). With the assumption that the intergalactic MF points towards the observer, we can derive the integral formula of $\mathrm{RM_{IGM}}$, which is larger than the actual values.

The redshifts of FRBs can be roughly constrained to be less than 1, according to the extragalactic contribution in Table 1 of $\mathrm{DM_E} \lesssim 10^3\ \mathrm{pc\ cm^{-3}}$ which corresponds to $z \sim 1$. We show in Figure 4 how both $\mathrm{DM_{IGM}}$ and $\mathrm{RM_{IGM}}$ evolve with z (between 0 and 1), where B_0 adopts the upper limit of 10^{-3} μG. As can be seen from Figure 4, $\mathrm{RM_{IGM}}$ is on the order of 1 $\mathrm{rad\ m^{-2}}$, which is negligible compared to the extragalactic components listed in Table 1.

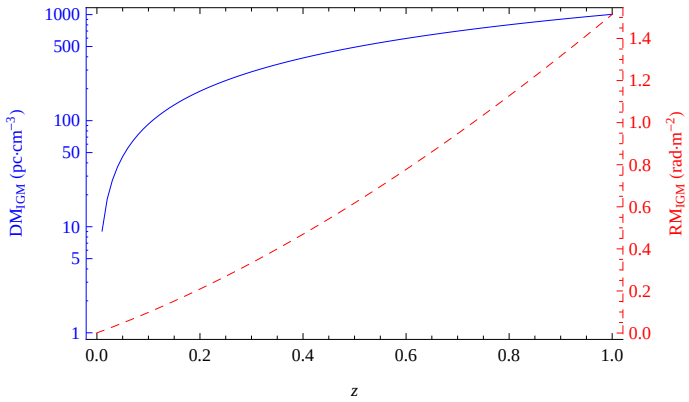

Fig. 4 $\mathrm{DM_{IGM}}$ (*blue solid line*) and $\mathrm{RM_{IGM}}$ (*red dashed line*) evolve with redshift z.

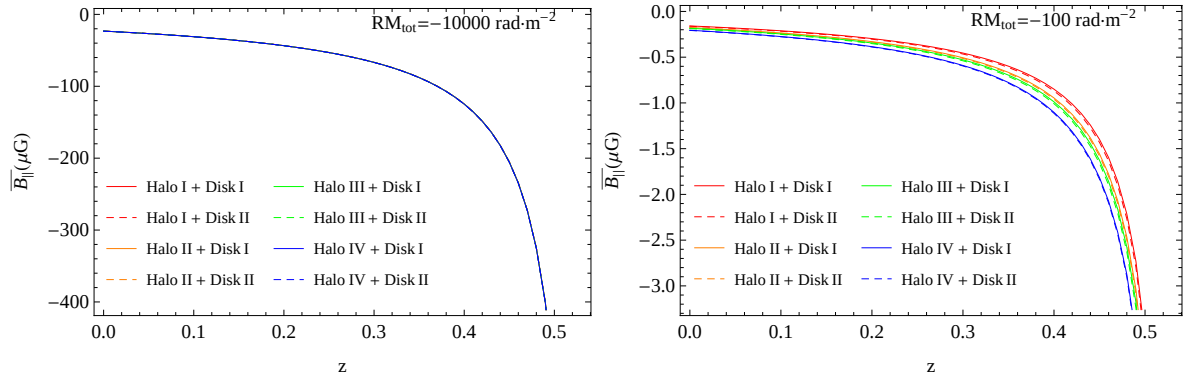

Fig. 5 The dependence on redshift of $\overline{B}_{||}$ for FRB 140514 when $\mathrm{RM_{tot}}$ is fixed to $-10\,000$ (*left*) and -100 rad m^{-2} (*right*). The parameters for Halo I are quoted from Sun et al. (2008).

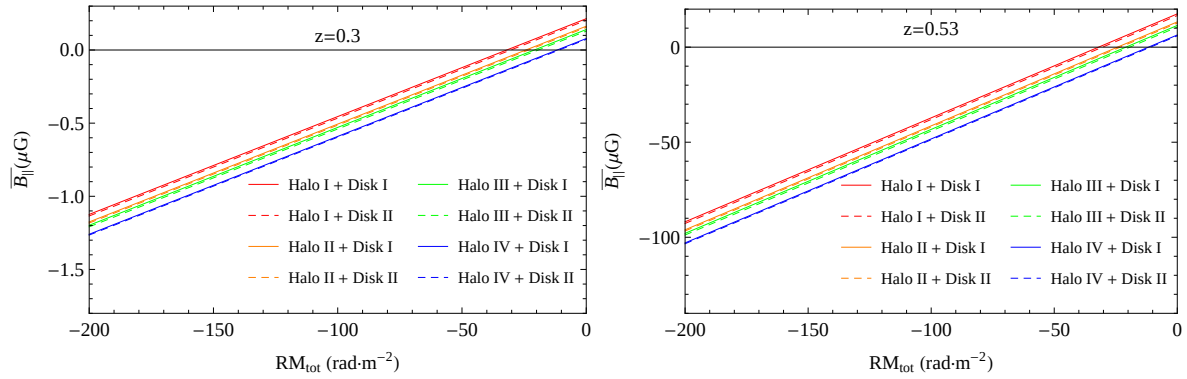

Fig. 6 The dependence on $\mathrm{RM_{tot}}$ of $\overline{B}_{||}$ for FRB 140514 when redshift is fixed to 0.3 (*left*) and 0.53 (*right*). The parameters for Halo I are quoted from Sun et al. (2008).

5 RESULTS AND DISCUSSIONS

Based on Equation (4) and Equation (5), we obtain the parallel MF component $\overline{B}_{||}$ averaged along the path where the radio wave propagates in the host galaxy

$$\begin{aligned}\overline{B}_{||} &= 1.23(1+z_{\rm host})\frac{\mathrm{RM_{host}}}{\mathrm{DM_{host}}} \\ &= 1.23(1+z_{\rm host})\frac{\mathrm{RM_{tot}}-\mathrm{RM_{MW}}}{\mathrm{DM_{tot}}-\mathrm{DM_{MW}}-\mathrm{DM_{IGM}}}, \quad (8)\end{aligned}$$

where $\mathrm{RM_{IGM}}$ is small enough to neglect. However, accurate values of $\mathrm{RM_{tot}}$ and redshift remain unavailable. If one of them is fixed, we could get the relationship between the parallel field component and the other quantity.

In the following, we take FRB 140514 as an example with constraints of redshift $z \lesssim 0.534$ and $|\mathrm{RM_{tot}}| \leqslant 1.18\times10^5$ rad m^{-2} (Petroff et al. 2015). We show $\overline{B}_{||}$ versus redshift for given $\mathrm{RM_{tot}}$ in Figure 5 and can see that the field strength increases monotonically with redshift. In particular as redshift approaches the limit where $\mathrm{DM_{host}}$ is

near zero, the field strength can approach infinity. The result for $\mathrm{RM_{tot}} = -10\,000\ \mathrm{rad\ m^{-2}}$ indicates that the dependence of field strength on different Galactic MF models can be neglected.

Figure 6 shows that $\overline{B}_{||}$ scales linearly with $\mathrm{RM_{tot}}$ when redshift is evaluated for both 0.3 and 0.53. Comparing the cases that have different redshifts, we find that the larger the redshift is, the faster $\overline{B}_{||}$ increases with $\mathrm{RM_{tot}}$. According to the above numerical calculation, $\overline{B}_{||}$ varies from $0.1\ \mu\mathrm{G}$ to several orders of magnitude higher than $1\ \mu\mathrm{G}$. Considering the fact that there are field reversals along the path, the numerical result is the lower limit on the field strength in the environment of FRBs. The MF observed in the hotspots and knots of active galactic nuclei (AGN) jets spans a similar range as our results (e.g., Zhang et al. 2010). It can be ruled out that the sources of FRBs are located in the extended regions of AGN because the spectra of AGN jets would overwhelm those of the FRBs.

As is well known, the MF significantly contributes to the structure of galaxies. The theory of MF equipartition implies that the energy density of MF is roughly equal to that of relativistic particles derived from galactic synchrotron luminosity (e.g., Govoni & Feretti 2004). In other words, this field strength reflects the injection rate of relativistic particles and the star formation rate, which is an important property to classify the galaxies. Beck (2009) listed the equipartition MF of different types of galaxies, e.g., about $5\ \mu\mathrm{G}$ for radio faint galaxies, 20–30 $\mu\mathrm{G}$ in the spiral arms of gas-rich spiral galaxies, and 50–100 $\mu\mathrm{G}$ for starburst galaxies. Thus we can constrain the type of galaxies that host FRBs by our results, i.e. the parallel field component. On the other hand, since the MF equipartition is derived from radio synchrotron emission, it mainly reflects the field component perpendicular to the line of sight (Han & Wielebinski 2002). Our results can be combined with the equipartition field to describe the rough 3D structure of an extragalactic field. Moreover, large $\overline{B}_{||}$ suggests a strong environmental MF. Then the search for FRBs can be narrowed down to a strong field. Conversely, it is an effective way to look for a strong field through the signals of FRBs.

In summary, we have shown that FRBs can act as a probe of their environmental field, which in turn provides a clue to unveiling mysterious FRBs. Since FRBs have a high event rate, we expect that observations in the future will offer more information that can be used to test the feasibility of our ideas and advance the study of FRBs.

Acknowledgements This work was supported by the National Basic Research Program ("973" Program) of China (Grant No. 2014CB845800) and the National Natural Science Foundation of China (Grant No. 11033002).

References

Beck, R. 2009, Astrophysics and Space Sciences Transactions, 5, 43
Burke-Spolaor, S., & Bannister, K. W. 2014, ApJ, 792, 19
Cordes, J. M., & Lazio, T. J. W. 2002, astro-ph/0207156
Cordes, J. M., & Lazio, T. J. W. 2003, astro-ph/0301598
Deng, W., & Zhang, B. 2014, ApJ, 783, L35
Dermer, C. D., Cavadini, M., Razzaque, S., et al. 2011, ApJ, 733, L21
Dolag, K., Kachelriess, M., Ostapchenko, S., & Tomàs, R. 2011, ApJ, 727, L4
Falcke, H., & Rezzolla, L. 2014, A&A, 562, A137
Fan, X., Carilli, C. L., & Keating, B. 2006, ARA&A, 44, 415
Govoni, F., & Feretti, L. 2004, International Journal of Modern Physics D, 13, 1549
Han, J. L., & Qiao, G. J. 1994, A&A, 288, 759
Han, J. L., Manchester, R. N., Berkhuijsen, E. M., & Beck, R. 1997, A&A, 322, 98
Han, J. L., Manchester, R. N., & Qiao, G. J. 1999, MNRAS, 306, 371
Han, J.-L., & Wielebinski, R. 2002, ChJAA (Chin. J. Astron. Astrophys.), 2, 293
Han, J. L., Manchester, R. N., Lyne, A. G., Qiao, G. J., & van Straten, W. 2006, ApJ, 642, 868
Inoue, S. 2004, MNRAS, 348, 999
Jansson, R., Farrar, G. R., Waelkens, A. H., & Enßlin, T. A. 2009, J. Cosmol. Astropart. Phys., 7, 21
Kashiyama, K., Ioka, K., & Mészáros, P. 2013, ApJ, 776, L39
Lorimer, D. R., Bailes, M., McLaughlin, M. A., Narkevic, D. J., & Crawford, F. 2007, Science, 318, 777
Mao, S. A., McClure-Griffiths, N. M., Gaensler, B. M., et al. 2012, ApJ, 755, 21
Neronov, A., & Vovk, I. 2010, Science, 328, 73
Petroff, E., Bailes, M., Barr, E. D., et al. 2015, MNRAS, 447, 246
Planck Collaboration, Ade, P. A. R., Aghanim, N., et al. 2014, A&A, 571, A16
Popov, S. B., & Postnov, K. A. 2007, arXiv:0710.2006
Prouza, M., & Šmída, R. 2003, A&A, 410, 1
Pshirkov, M. S., Tinyakov, P. G., Kronberg, P. P., & Newton-McGee, K. J. 2011, ApJ, 738, 192
Ruiz-Granados, B., Rubiño-Martín, J. A., & Battaner, E. 2010, A&A, 522, A73
Rybicki, G. B., & Lightman, A. P. 1979, Radiative Processes in Astrophysics (New York: Wiley-Interscience)
Schleicher, D. R. G., & Miniati, F. 2011, MNRAS, 418, L143
Spitler, L. G., Cordes, J. M., Hessels, J. W. T., et al. 2014, ApJ, 790, 101
Sun, X.-H., & Reich, W. 2010, RAA (Research in Astronomy and Astrophysics), 10, 1287
Sun, X. H., Reich, W., Waelkens, A., & Enßlin, T. A. 2008, A&A, 477, 573
Thornton, D., Stappers, B., Bailes, M., et al. 2013, Science, 341, 53
Totani, T. 2013, PASJ, 65, L12
Vallee, J. P. 1975, Nature, 254, 23
Zhang, B. 2014, ApJ, 780, L21
Zhang, J., Bai, J. M., Chen, L., & Liang, E. 2010, ApJ, 710, 1017